Thermal Conductivity of Single-Walled Carbon Nanotube with Internal Heat Source Studied by Molecular Dynamics Simulation

Yuan-Wei Li & Bing-Yang Cao

International Journal of Thermophysics
Journal of Thermophysical Properties and Thermophysics and Its Applications

ISSN 0195-928X
Volume 34
Number 12

Int J Thermophys (2013) 34:2361-2370
DOI 10.1007/s10765-011-1004-0

Springer

Int J Thermophys (2013) 34:2361–2370
DOI 10.1007/s10765-011-1004-0

Thermal Conductivity of Single-Walled Carbon Nanotube with Internal Heat Source Studied by Molecular Dynamics Simulation

Yuan-Wei Li · Bing-Yang Cao

Received: 27 December 2010 / Accepted: 11 May 2011 / Published online: 26 May 2011

Abstract The thermal conductivity of (5, 5) single-walled carbon nanotubes (SWNTs) with an internal heat source is investigated by using nonequilibrium molecular dynamics (NEMD) simulation incorporating uniform heat source and heat source-and-sink schemes. Compared with SWNTs without an internal heat source, i.e., by a fixed-temperature difference scheme, the thermal conductivity of SWNTs with an internal heat source is much lower, by as much as half in some cases, though it still increases with an increase of the tube length. Based on the theory of phonon dynamics, a function called the phonon free path distribution is defined to develop a simple one-dimensional heat conduction model considering an internal heat source, which can explain diffusive-ballistic heat transport in carbon nanotubes well.

Keywords Internal heat source · Phonon dynamics · Single-walled carbon nanotubes · Thermal conductivity

1 Introduction

Since the discovery of carbon nanotubes (CNTs) by Iijima in 1991 [1], CNTs have attracted much attention because of their extraordinary electrical, mechanical, and thermal properties [2]. As one of the most important properties, the thermal conductivity of CNTs has been studied by experimental measurements [3–6], theoretical analyses [7,8], and molecular dynamics (MD) simulations [9–12]. The thermal

Y.-W. Li · B.-Y. Cao (✉)
Key Laboratory for Thermal Science and Power Engineering of Ministry of Education, Department of Engineering Mechanics, Tsinghua University, Beijing 100084, People's Republic of China
e-mail: caoby@tsinghua.edu.cn

Y.-W. Li
e-mail: liyuanwei66@163.com

conductivities of single-walled carbon nanotubes (SWNTs) and multi-walled carbon nanotubes (MWNTs) were measured in [3,4] and [5,6], respectively, and gave a range of 2 000 $W \cdot m^{-1} \cdot K^{-1}$ to 3 500 $W \cdot m^{-1} \cdot K^{-1}$. It should be noted that the method used in [6] is a self-heating scheme, while for most other previous studies, including experimental measurements, theoretical analyses, and MD simulations, the thermal conductivity is studied based on a fixed-temperature difference or heat flux scheme. However, CNTs have a quasi-one-dimensional structure, and the thermal conductivity, i.e., the process of heat (phonons) transport, is dependent on the tube length. One potential application of CNTs is in electrical management due to their excellent electrical properties, where the thermal transport may be different for conditions without an internal heat source. In this case, the contribution of the ballistic phonons to the thermal transport is directly related to the position of the internal heat source, and Fourier's law of heat conduction breaks down. To the best of our knowledge, the application of the uniform heat source (UHS) scheme to CNTs has not been reported. Furthermore, the thermal conductivity of CNTs with an internal heat source has not been studied.

The thermal conductivity of SWNTs with an internal heat source is investigated by using nonequilibrium molecular dynamics (NEMD) simulations in this article. It shows that, although the thermal conductivity of SWNTs increases with an increase of the tube length because of diffusive-ballistic phonon transport, the present results are always lower compared with previous results without an internal heat source. Based on phonon dynamics, we put forward a function called the phonon free path distribution to derive a simple one-dimensional heat conduction model, which characterizes the thermal transport in CNTs with an internal heat source well.

2 Molecular Dynamics Simulation

The heat source-and-sink (HSS) [13] and UHS schemes are employed to study the thermal conductivity of (5, 5) SWNTs with an internal heat source. The fixed-temperature difference (FTD) scheme is also given in this article for comparison.

The bond-order potential presented by Brenner [14] is used to describe the atomic interactions,

$$E = \sum_i \sum_{j(>i)} \left[V_{\mathrm{R}}\left(r_{ij}\right) - b_{ij} V_{\mathrm{A}}\left(r_{ij}\right) \right], \tag{1}$$

where $V_{\mathrm{R}}(r)$ and $V_{\mathrm{A}}(r)$ denote the repulsive and attractive interactions, respectively, and b_{ij} is the bond-order term. The bond length $a_{\mathrm{cc}} = 1.44$ Å, wall thickness $\delta = 0.34$ Å, and cross-section area $S = 2\pi R\delta$, in which R is the radius of the nanotube. The motion equations of atoms are integrated by a leap-frog scheme [15] with a 0.5 fs time step. For all simulation cases in this article, the system requires 2 000 000 time steps to reach a steady state, and then 3 000 000 time steps to average the temperature profile and heat source density.

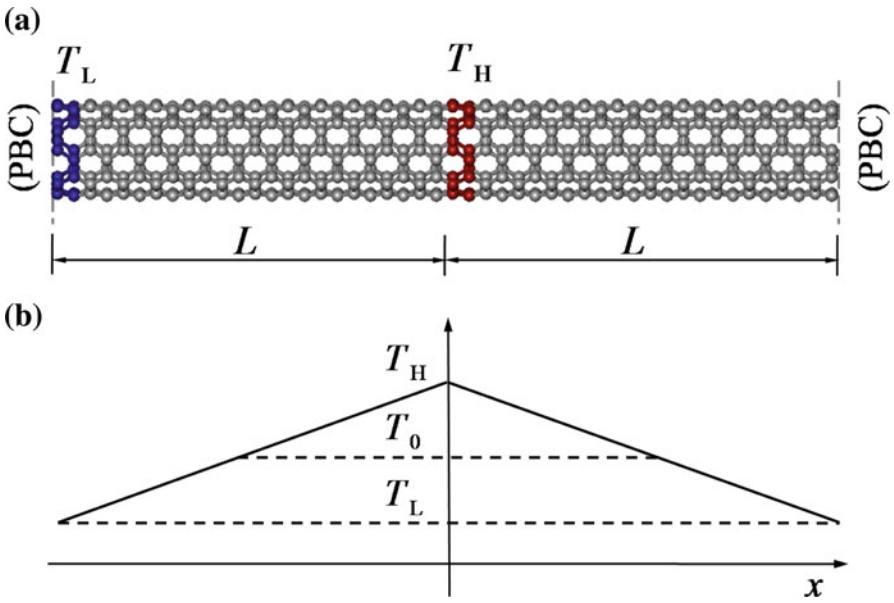

Fig. 1 (a) Schematic of the FTD simulation system and (b) symmetrical linear temperature profile due to periodic boundary conditions

2.1 Fixed-Temperature Difference Scheme

The FTD scheme is illustrated in Fig. 1, which contains a high-temperature slab and a low-temperature slab whose temperatures are controlled by the Nose–Hoover thermostat [16]. A symmetrical linear temperature distribution is obtained due to periodic boundary conditions. The thermal conductivity can be defined by Fourier's law of heat conduction,

$$\lambda = -q/\nabla T, \tag{2}$$

where λ is the thermal conductivity, q is the heat flux density, and T is the local temperature. Additional details about the FTD scheme can be found in previous study by Hou et al. [12].

2.2 Heat Source-and-Sink Scheme

The system simulated by the HSS scheme [13] is divided identically into a heat sink region and a heat source region, as shown in Fig. 2. The uniform heat sink and source are obtained simultaneously by the velocity vector exchange method developed by Müller-Plathe [17]. The exchanges of the vectors of atoms i, j are to remove energy from the sink region while injecting energy into the source region, keeping the heat source and sink uniform and the total energy and momentum of the system conserved. The heat source and sink densities can be obtained as

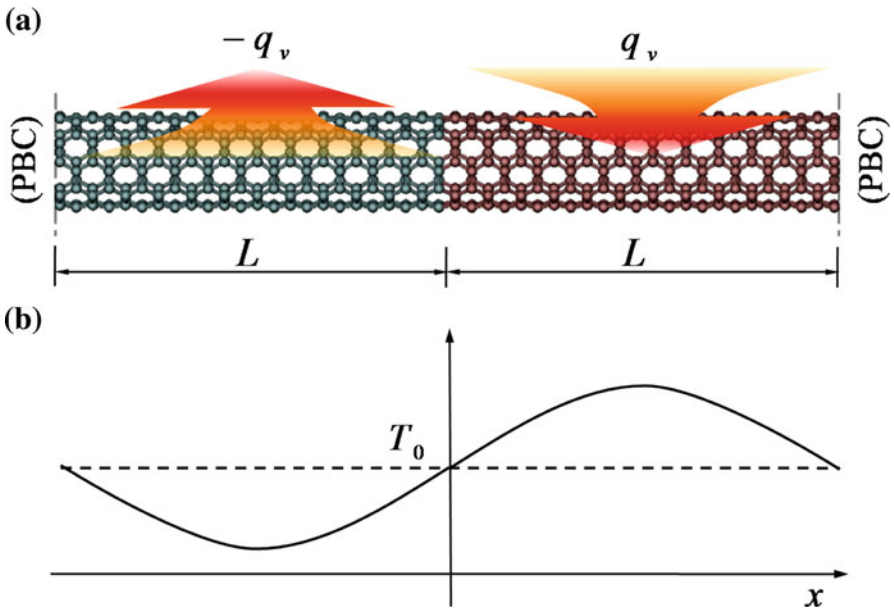

Fig. 2 (a) Schematic of the HSS simulation system including a heat sink region (*left half*) and a source region (*right half*) and (b) periodically quadratic temperature profile for periodic boundary conditions

$$q_v = \frac{\sum\limits_{\text{transfers}} \frac{m}{2}\left(v_i^2 - v_j^2\right)}{tSL}, \tag{3}$$

where v_i, v_j are the velocities of atom i, j, respectively, m is the atomic mass, t is the statistical time, and L is half of the system length. The temperature profile can be derived from Fourier's law of heat conduction,

$$T(x) = \begin{cases} \frac{q_v}{2\lambda}\left(x + \frac{L}{2}\right)^2 - \frac{q_v L^2}{8\lambda} + T_0 & (-L \le x < 0) \\ -\frac{q_v}{2\lambda}\left(x - \frac{L}{2}\right)^2 + \frac{q_v L^2}{8\lambda} + T_0 & (0 < x \le L) \end{cases}, \tag{4}$$

where T_0 is the average temperature of the system. The thermal conductivity can be extracted from the mean temperatures of the sink and source regions, i.e., $\overline{T_{\mathrm{L}}}$, $\overline{T_{\mathrm{R}}}$,

$$\lambda = \frac{q_v L^2}{12\,\overline{\Delta T}}, \tag{5}$$

where $\overline{\Delta T} = \left[\left(T_0 - \overline{T}_{\mathrm{L}}\right) + \left(\overline{T}_{\mathrm{R}} - T_0\right)\right]/2$, which is kept lower than 20 K by controlling the exchange interval time steps in all of our simulation cases. The thermal conductivity can also be obtained by fitting the temperature distribution curve, which will be stated in the UHS scheme in the next section.

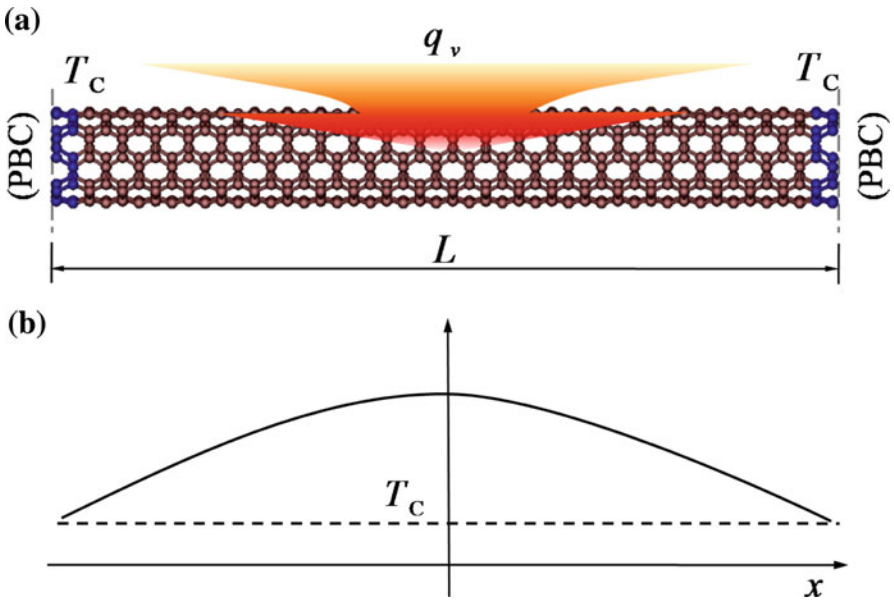

Fig. 3 (a) Schematic of the UHS simulation system, two ends are thermostated to a constant temperature, while energy is injected into the remaining part uniformly and (b) the quadratic temperature profile for periodic boundary condition

2.3 Uniform Heat Source Scheme

The simulation system for the UHS scheme is shown in Fig. 3. The temperature of the two ends is maintained at a constant $T_C (T_C = T_0)$ by the Nose–Hoover thermostat [16]. Similar to the self-heating method in [6], the UHS is obtained by modifying the velocity vectors of atoms i, j while keeping the total momentum conserved. The heat source density can be given as

$$q_v = \frac{\sum\limits_{\text{modifys}} \frac{m}{2}\left[\left(v_i^{n2} - v_i^{o2}\right) + \left(v_j^{n2} - v_j^{o2}\right)\right]}{tSL}, \tag{6}$$

in which v_i^{o}, v_i^{n}, v_j^{o}, v_j^{n} are the old and new velocities of atoms i, j. The temperature profile can be derived from Fourier's law of heat conduction

$$T(x) = -\frac{q_v}{2\lambda}x^2 + \frac{q_v L^2}{8\lambda} + T_C. \tag{7}$$

Several additional phonon modes may be excited by the thermostat and lead to the boundary temperature jumps [18]. The mean temperature method (similar to the HSS scheme) to extract the thermal conductivity is not suitable. Therefore, the thermal conductivity is calculated by fitting the temperature distribution,

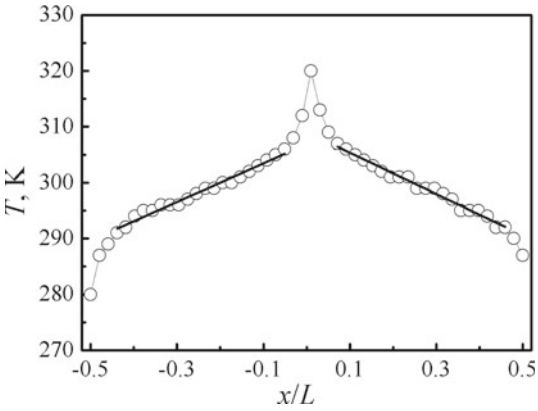

Fig. 4 Temperature profiles by the FTD scheme: *open circles* are obtained by NEMD and *solid line* is fitted based on the calculated data

$$\lambda = -q_v/2a, \tag{8}$$

in which a is the quadratic coefficient of the fitted temperature curve.

3 Results and Discussion

3.1 Temperature Distribution

The thermal conductivity by the FTD scheme can be obtained by Fourier's law of heat conduction by using the linear temperature distribution as shown in Fig. 4, while the mean temperature difference method is used to calculate the thermal conductivity for the HSS scheme and the fitting method is applied for the UHS scheme. For the HSS scheme, when using the thermal conductivity obtained by the method of the mean temperatures of the left-half and right-half systems to predict the temperature profile, we find that the predicted temperature curve (HSS1 in Fig. 5) slightly deviates from the practical temperature distribution (HSS2, the fitted curve of the calculated data). The predicted mean temperature difference is larger than the practical one, which means that the predicted thermal conductivity is lower than the practical one. It also indicates that the thermal conductivity is not a constant any longer, and the concept of "local thermal conductivity" may not be rational. For the UHS scheme, the temperature distribution can be well described by the fitting curve regardless of the boundary jumps, as shown in Fig. 6, which means that the local thermal conductivities along the tube may be a constant.

3.2 Thermal Conductivity

The dependence of the thermal conductivity of SWCNTs on the tube length for different schemes is shown in Fig. 7. All the thermal conductivities obtained by different methods increase with an increase of the tube length, which reflects the ballistic transport of phonons in the CNTs. However, the increase rates are not the same for different

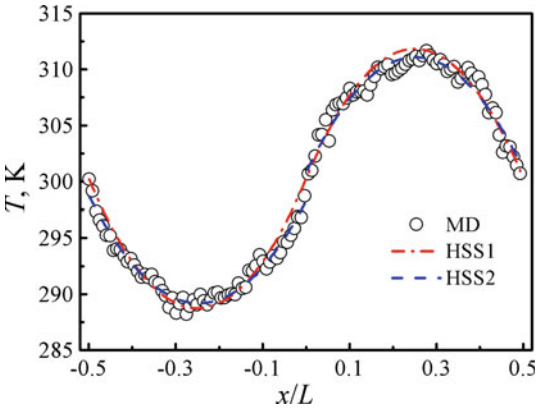

Fig. 5 Temperature profiles by the HSS scheme: *open circles* are obtained by NEMD, *dashed-dotted curve* is predicted by the thermal conductivity extracted according to the mean temperature method, and *dashed curve* is fitted based on the calculated data

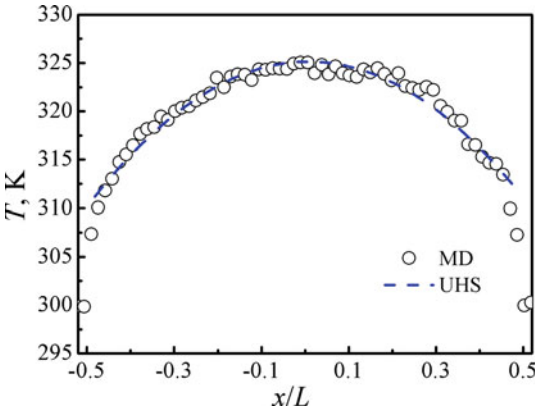

Fig. 6 Temperature profiles by the UHS scheme: *open circles* are obtained by NEMD and *dashed curve* is fitted based on the calculated data

methods. The thermal conductivity by the FTD method increases from 34 $W \cdot m^{-1} \cdot K^{-1}$ at 6 nm to 360 $W \cdot m^{-1} \cdot K^{-1}$ at 100 nm, but the thermal conductivities calculated by the HSS and UHS methods are much lower. For the HSS scheme, the thermal conductivity obtained by the mean temperature difference method (HSS1) is from 21 $W \cdot m^{-1} \cdot K^{-1}$ at 6 nm to 239 $W \cdot m^{-1} \cdot K^{-1}$ at 100 nm, and that by fitting the temperature profile (HSS2), ranges from 27 $W \cdot m^{-1} \cdot K^{-1}$ at 6 nm to 287 $W \cdot m^{-1} \cdot K^{-1}$ at 100 nm. Furthermore, the thermal conductivity obtained by the UHS scheme by a curve fitting method (UHS) ranges only from 23 $W \cdot m^{-1} \cdot K^{-1}$ at 6 nm to 194 $W \cdot m^{-1} \cdot K^{-1}$ at 100 nm. According to the simulation results, we can draw the following conclusions. First, when there is an internal heat source or sink in CNTs, different simulation schemes give different thermal conductivities. Even for the HSS method, the mean temperature difference and fitting temperature curve methods give different thermal conductivities. Second, the thermal conductivity for CNTs with an internal heat source or sink is always lower than that with a FTD, even by half in some cases. It implies that it is a crucial problem to define the thermal conductivity of CNTs with an internal heat source or sink. Third, the essential point is that the thermal transport in CNTs is in a diffusive-ballistic way. In this case, Fourier's law of heat conduction breaks down.

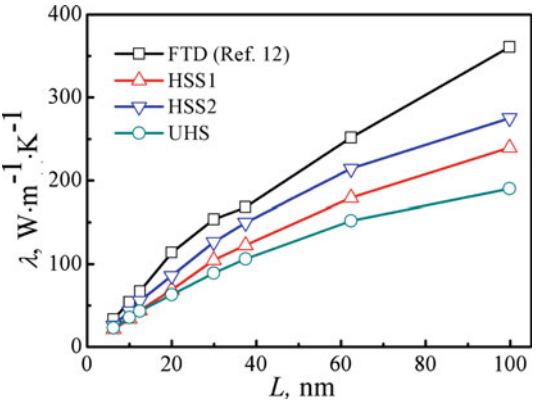

Fig. 7 Length dependence of the thermal conductivity of SWNTs

Hence, the heat conduction model based on the phonon kinetics should be taken into account.

4 Analyses Based on Phonon Dynamics

The mean free path (MFP) of phonons is an important concept for understanding the heat conduction in CNTs, and the thermal conductivity of CNTs can be expressed as

$$\lambda = C v_{\mathrm{g}} \bar{l}, \tag{9}$$

where C is the specific heat, v_{g} is the phonon group velocity, and $\bar{l}$ is the phonon MFP, which is an energy-weighted mean free path instead of just an average quantity due to the diversity of phonons. A function of the energy-weighted free path distribution $\Theta(l)$ is hereby defined as

$$\Theta\,(l) = \frac{\mathrm{d}Q}{Q\mathrm{d}l}, \tag{10}$$

in which l is the phonon free path, Q is the total energy of all phonons, and $\mathrm{d}Q$ is the energy for $l \in [l,\ l + \mathrm{d}l)$. As a distribution function, $\Theta(l)$ must satisfy $\Theta(l) \geq 0$, $\Theta(0) = \Theta(\infty) = 0$, and $\int_0^\infty \Theta\,(l)\,\mathrm{d}l = 1$. Since "for phonons traveling through a defect-free nanotube, the only scattering mechanisms are due to lattice anharmonicity" [8], and combined with the Boltzmann–Peierls phonon transport equation [19], we conclude that $\Theta(l)$ is related to the temperature but not to the tube length, and it reveals an intrinsic property of CNTs. For an infinite system, the phonon MFP $\bar{l}$ can be obtained by

$$\bar{l} = \int_0^\infty \Theta\,(l)\,l\mathrm{d}l. \tag{11}$$

While for a finite system L, the phonons with $l \geq L$ will show $l = L$ due to the tube length limitation, i.e., boundary scattering. Then we have

$$\bar{l} = \int_0^L \Theta(l)\, l\, \mathrm{d}l + L \int_L^\infty \Theta(l)\, \mathrm{d}l. \tag{12}$$

The derivative of Eq. 12 can be written as

$$\frac{\mathrm{d}\bar{l}}{\mathrm{d}L} = \int_L^\infty \Theta(l)\, \mathrm{d}l > 0. \tag{13}$$

It shows that $\bar{l}$ increases with an increase of the tube length L, but the increase in the rate will decrease as the tube length increases. Equation 12 also shows that $\bar{l}$ is always smaller than L, but will approach L when L becomes very small, which also can be obtained by Matthiessen's rule,

$$\bar{l}^{-1} = \bar{l}_{\mathrm{p-p}}^{-1} + L_{\mathrm{et}}^{-1}, \tag{14}$$

where $\bar{l}_{\mathrm{p-p}}$ is the phonon MFP in Umklapp scattering, which is approximately a constant, and L_{et} is the distance of energy transport. Reference [5] reported that the phonon MFP $\bar{l}$ was about 0.75 μm for a 2.76 μm length and 1 nm diameter SWNTs at 300 K, which means the phonon MFP in Umklapp scattering is about 1 μm. Since the diameter of a single-walled CNT (5, 5) is about 0.69 nm, $\bar{l}_{\mathrm{p-p}}$ should be larger than 1 μm. For the FTD scheme, $L_{\mathrm{et}} \approx L$, simplify $\bar{l}$ as $\bar{l} \approx L$ for L in the range of 0 to 100 nm, and the thermal conductivity can be described as

$$\lambda \approx C v_{\mathrm{g}} L. \tag{15}$$

For the UHS system with an internal heat source, the phonons can be grouped as left-phonons (moving to the left) and right-phonons (moving to the right), whose distance of energy transport L_{et} can be considered as x and $L - x$, respectively. Because of the independence on L for $\Theta(l)$ and the symmetry of phonon motions, the functions of the phonon free path for the left-phonons $\Theta_{\mathrm{L}}(l)$ and right-phonons $\Theta_{\mathrm{R}}(l)$ have a relationship of $\Theta_{\mathrm{L}}(l) = \Theta_{\mathrm{R}}(l) = \Theta(l)$. Then, the left-phonon MFP $\bar{l}_{\mathrm{L}}$ and right-phonon MFP $\bar{l}_{\mathrm{R}}$ can also be simplified as $\bar{l}_{\mathrm{L}} \approx x$ and $\bar{l}_{\mathrm{R}} \approx L - x$, respectively. The distribution of the phonon MFP along the tube can be described as $\bar{l}(x) = \left(\bar{l}_{\mathrm{L}} + \bar{l}_{\mathrm{R}}\right)/2 \approx L/2 = \text{constant}$, which is consistent with the results of the UHS scheme. Therefore, the average phonon MFP along the tube using a weighted energy transport (heat source density) is given as

$$\bar{l} = \frac{1}{L} \int_0^L \bar{l}(x)\, \mathrm{d}x \approx \frac{1}{2} L. \tag{16}$$

Since the temperature difference of the system is small and the phonon group velocity can be assumed as $v_g \approx$ constant. Then the average thermal conductivity along the tube can be described as

$$\overline{\lambda} \approx \frac{1}{2} C v_g L. \tag{17}$$

It shows that the thermal conductivity of the UHS simulation system with an internal heat source is nearly half of that of the FTD simulation system without a heat source, which is approximately consistent with the simulation results for the SWNT length in the range of 10 nm to 100 nm as shown in Fig. 7.

5 Conclusions

The thermal conductivity of (5, 5) SWNTs with an internal heat source is investigated by using NEMD simulations based on UHS and HSS schemes. Though the thermal conductivity of SWNTs with an internal heat source increases with an increase of the tube length as predicted by diffusive-ballistic phonon kinetics, the present results are found to be smaller than those of SWNTs with a fixed-temperature difference or heat flux, even by half in some cases. Based on the theory of phonon dynamics, a function called the phonon free path distribution is defined to develop a simple one-dimensional heat conduction model considering an internal heat source, which can well explain diffusive-ballistic heat transport in CNTs.

Acknowledgments This study is financially supported by the National Natural Science Foundation of China (No. 50976052, 50606018, 50730006) and the Tsinghua National Laboratory for Information Science and Technology (TNList) Cross-discipline Foundation.

References

1. S. Iijima, Nature **354**, 56 (1991)
2. R.H. Baughman, A.A. Zakhidov, W.A. Heer, Science **297**, 787 (2002)
3. P. Kim, L. Shi, A. Majumdar, P.L. McEuen, Phys. Rev. Lett. **87**, 215502 (2001)
4. M. Fujii, X. Zhang, H.Q. Xie, H. Ago, K. Takahashi, T. Ikuta, Phys. Rev. Lett. **95**, 065502 (2005)
5. C. Yu, L. Shi, Z. Yao, D.Y. Li, A. Majumdar, Nanotechnol. Lett. **5**, 1842 (2005)
6. E. Pop, D. Mann, Q. Wang, K. Goodson, H.J. Dai, Nanotechnol. Lett. **6**, 96 (2006)
7. J.X. Cao, X.H. Yan, Y. Xiao, J.W. Ding, Phys. Rev. B **69**, 073407 (2004)
8. N. Mingo, D.A. Broido, Nanotechnol. Lett. **5**, 1221 (2005)
9. S. Berber, Y.K. Kwon, D. Tomanek, Phys. Rev. Lett. **84**, 4613 (2000)
10. B.W. Li, J. Wang, L. Wang, G. Zhang, Chaos **15**, 015121 (2005)
11. K.D. Bi, Y.F. Chen, J.K. Yang, Y.J. Wang, M.H. Chen, Phys. Lett. A **350**, 150 (2005)
12. Q.W. Hou, B.Y. Cao, Z.Y. Guo, Acta Phys. Sin. **58**, 7809 (2009) (in Chinese)
13. B.Y. Cao, Y.W. Li, J. Chem. Phys. **133**, 024106 (2010)
14. D.W. Brenner, Phys. Rev. B **42**, 9458 (1990)
15. M.P. Allen, D.J. Tildesley, *Computer Simulation of Liquids* (Oxford University, New York, 1989)
16. W.G. Hoover, Phys. Rev. A **31**, 1695 (1985)
17. F. Müller-Plathe, J. Chem. Phys. **106**, 6082 (1997)
18. J.W. Jiang, J. Chen, J.S. Wang, B.W. Li, Phys. Rev. B **80**, 052301 (2009)
19. R.E. Peierls, *Quantum Theory of Solids* (Oxford University, New York, 1955)